Polymer Degradation and Stability 144 (2017) 137–145

Contents lists available at ScienceDirect

Polymer Degradation and Stability

journal homepage: www.elsevier.com/locate/polydegstab

Water diffusion and swelling stresses in ionizing radiation cured epoxy matrices

Sabina Alessi*, Andrea Toscano, Giuseppe Pitarresi, Clelia Dispenza, Giuseppe Spadaro

Università degli Studi di Palermo, Dipartimento dell'Innovazione Industriale e Digitale (DIID), Viale delle Scienze, 90128 Palermo, Italy

ARTICLE INFO

Article history:
Received 18 May 2017
Received in revised form
13 July 2017
Accepted 10 August 2017
Available online 12 August 2017

Keywords:
Epoxy resins
Radiation curing
Hydrothermal aging
Swelling
Dynamic mechanical thermal analysis
Photoelastic Stress Analysis

ABSTRACT

In this work a DGEBF epoxy monomer was cured by electron beam radiation in the presence of an iodonium salt and the obtained system was hydrothermally aged as such and also after a thermal treatment, in order to obtain two systems having different uniformity in the cross-linking degree. On both systems, the transient stress field arising from swelling was measured and monitored by an optical Photoelastic technique and the results were commented with reference to a thermally cured epoxy system containing the same monomer and already discussed in a previous work. Beam samples with identical dimensions, obtained from the irradiated systems, have been aged at 80 °C in water, and characterised by Gravimetric and DMTA tests. The results are compared also with already reported swelling behaviour of similar thermally cured systems. It is observed that the different curing techniques (radiation curing, radiation curing followed by thermal curing and thermal curing) determine a different network structure and a different water chemical affinity, which influence the amounts of absorbed/desorbed water, and the relative amounts of bonded/free water. Such differences affect the swelling behaviour, and then the transient stress field. Photoelastic Stress Analysis has allowed to evaluate the evolving stress field, providing a different point of view on the investigation of the material transformations associated to water diffusion.

1. Introduction

Thermoset resins are used in various structural applications such as matrices for composites, adhesive joining and coatings. Traditional manufacturing processes use thermal curing of epoxy monomers and/or oligomers in presence of various curing agents [1–4], with a certain ability to tailor physical/mechanical properties such as glass transition temperature, toughness and strength [4–7].

Alternative to thermal process, curing by interaction of ionizing radiation with apt epoxy formulations has been studied [8–13], due to some potential advantages with respect to the more traditional thermal process. In fact, ionizing radiation curing of epoxy resin can be an environmentally friendly process, due to the possibility to work at mild temperatures and without the use of organic solvents. Furthermore, also the mechanical properties can be improved due to the reduced presence of thermally induced stresses during curing processing.

An important requirement of epoxy resins based materials for structural applications is their ability to maintain the properties within a fixed range during their operative life, i.e. to show significant resistance to the external aging factors such as thermal cycles, water or in general solvents absorption and desorption, etc. [14–18]. Among them, one of the more frequent ageing conditions is hydrothermal ageing, due to both temperature cycles and water absorption-desorption. In fact, water absorption induces some important transformation in the mechanical behaviour of epoxies. These include plasticization and degradation of the network structure, which may affect the strength and fracture toughness [19,20], and swelling, which may induce important internal stresses [21].

It is accepted that the absorbed water is partly filled in the polymer free volume and partly chemically bonded to the matrix [22]. The relative amount of bonded and free water and the role of each type of water in both swelling and degradation phenomena is more complex to establish due to the mutual influence of several factors. Some authors have suggested that the bonded water is the main responsible for swelling [22–24], since such bonds are usually bulkier than normal interchain hydrogen bonds [23], and Type I hydrolysis decreases Van Der Waals interchain forces [22]. On the

* Corresponding author. Tel.: +39 091 23863711; fax: +39 091 23860840.
E-mail address: sabina.alessi@unipa.it (S. Alessi).

http://dx.doi.org/10.1016/j.polymdegradstab.2017.08.009
0141-3910/

other hand, the formation of bonded water may induce changes in the network structure of the resin, which may also affect the free volume, and then the free water [4,25]. This changing scenario leads to modifications in water absorption which may affect the transitory as well as the final (equilibrium) properties of the aging material in ways that are difficult to predict [17].

The concurrent mechanisms of swelling/un-swelling during water absorption/desorption cycles are also particularly difficult to investigate, due to the several mutual effects occurring, and to a lack of reliable and simple measuring techniques. Hence, only few works in the scientific literature have attempted to investigate such transitory stages [21,25,26]. Some of the authors have recently proposed a new approach to evaluate the transitory swelling/un-swelling stresses, by means of Photoelastic Stress Analysis [21,27]. This technique, applied on thermally cured and differently cross-linked epoxy resin systems, has resulted in a robust method able to detect and monitor swelling stresses arising in transparent and birefringent samples. In this way, it is possible to evaluate the material in terms of its propensity to swell and to develop internal stresses, correlating this property to the kinetics of water uptake and to the thermal and mechanical properties of epoxy resin systems [27]. Furthermore, Photoelasticity is an ideal tool for evaluating the aptitude of a thermoset resin system to develop hygroscopic internal stresses from non-uniform swelling distributions, as can exist in water transport transients, or at the interface of different materials/phases.

The present work performs the Photoelastic analysis on two epoxy resin systems made with the same DGEBF monomer, subjected to hydrothermal aging up to equilibrium, followed by desorption in a room temperature dry airborne environment. Both monitored systems are cured by ionizing radiation, and one is further treated with a thermal post-cure. These different preparations determine different network structures, and then different water physical/chemical affinities, which influence the amounts of water absorbed/desorbed, and the relative amounts of bonded/free water. Such differences affect the swelling behaviour, and the relative transient stress fields. Results are then compared with the photoelastic response of the same monomer cured by traditional thermal curing and already presented in a previous study [27].

2. Experimental procedure

2.1. Materials and sample preparation

The epoxy monomer is based on Bis(4-glycidyloxyphenil) methane (DGEBF), (epoxide equivalent weight, 160–170), provided by Sigma Aldrich. For radiation curing an onium salt, cumyltolyliodonium tetra(pentafluorophenil) borate (Rh 2047) supplied by Rhodia Silicones, was used as initiator. The chemical formula of the relative components are reported in Fig. 1.

The epoxy monomer was compounded with 0.1 phr of the iodonium salt at 60 °C and stirred for about 30 min until the initiator was dissolved in the resin. E-beam irradiation was carried out, in steel moulds 150 × 150 mm, at the ISOF-CNR laboratory in Bologna, Italy, with the 12 MeV Vickers type linear accelerator whose technical characteristics are reported elsewhere [28]. The irradiation dose rate was 80 kGy/h and the total dose was 100 KGy. The resin blend was casted into an aluminium open mould flat plate, having a smooth finish needed for preserving the sufficient optical transparency required by the photoelastic analysis. During irradiation the temperature of the polymerizing resin has been recorded through a thermo resistor wired to a data acquisition system interfaced to a computer. The thermal profile, here not reported, revealed a temperature during irradiation always lower than 60 °C.

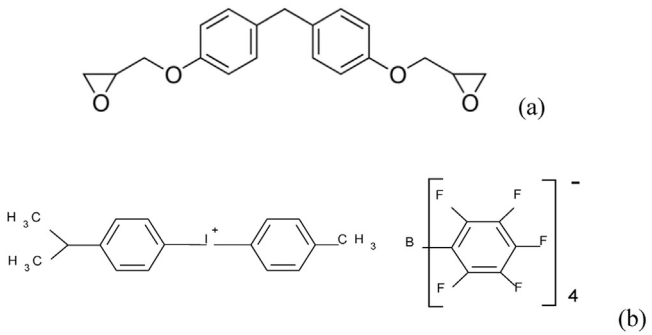

Fig. 1. Molecular structure of DGEBF monomer (a), Rh initiator (b).

After radiation cure, beam samples with nominal dimension of 36 × 8 × 3 mm were cut from the cured panels. Two lots of beam samples were considered, one radiation cured (DGEBFirr) and another thermally post cured in oven at 120 °C for 2 h after irradiation (DGEBFirr-pc). The choice of the DGEBF monomer is made in order to compare the outcomes of the present characterisation with the results from Ref. [27], where the same monomer is used and equivalent sample beams prepared by thermal curing (hereinafter referred as DGEBFt). DGEBFt was obtained curing the monomer by a tertiary ammine in a thermal cycle at high temperature and post curing the product material at 180 °C for 2 h. These treatments give rise to a highly crosslinked structure.

Care was taken in order to prepare and pre-condition all sample batches in a most similar way. Photoelastic Stress Analysis (see section 2.4) was used throughout each preparation step, to monitor the potential rise of internal stresses during cutting operations or while exposing the samples to the working environment before starting the hydrothermal aging. The following preparation procedure was in particular implemented:

1) Cured panels of all three batches were cut into beam sample shape on a table saw;
2) DGEBFirr-pc and DGEBFt beam samples were post-cured in a controlled oven. After the maximum post-cure temperature was reached, samples were brought back to room temperature with a very slow cooling of 24 h to avoid thermally induced residual stresses;
3) The three batches of samples (the two post-cured and the one simply cured), were then left for at least 24 h in a sealed container containing calcium chloride salt, before entering the hydrothermal aging bath.

Photoelasticity revealed that no meaningful internal stresses were introduced at the end of each of the three steps mentioned above.

2.2. Hydrothermal conditioning and gravimetric analysis

Hydrothermal aging of all cured samples has been carried out in deionised water at controlled temperature of 80 °C for a total time of about 1530 h. Desorption has been performed at room temperature (maintained almost constant at 25 °C) in a small sealed recipient (about 10^3 cm^3) with a relatively high content of calcium chloride salt to assure a dry airborne environment. In fact, in this condition, the atmospheric moisture is not in equilibrium, since the water vapour present in the air is not sufficient to the deliquescence of calcium chloride.

For the photoelastic and gravimetric characterizations, the specimens have been temporarily taken out of the bath a number of

times, throughout the duration of water sorption and desorption, with a higher frequency in the initial stages of both absorption and desorption. During these occasions, the samples have been wiped off of surface water, and successively left to rest at room temperature for about a minute. Finally, they have been weighed on a 0.01 mg resolution electronic balance for the gravimetric analysis, and placed in the polariscope for the acquisition of photoelastic images. The weighing results have been plotted in terms of percentage of mass uptake M_r versus time t, according to the follow equation:

$$M_r(t) = (M(t) - M(0))/M(0) \quad (1)$$

where $M(t)$ is the weight at the time t, $M(0)$ is the initial weight before the hydrothermal aging.

The gravimetric analysis, in the absorption and desorption process, has been carried out until no further significant mass change was observed.

2.3. Dynamic-mechanical-thermal analysis

Dynamic-mechanical-thermal analysis has been performed by a Rheometrics DMTA V apparatus, equipped with a three point bending fixture, in a temperature swift mode, in the 20–300 °C range at a heating rate of 10 °C/min. The strain level was set at 0.02% and the frequency was 1.8 Hz. Storage modulus (E') and loss factor ($\tan\delta$) versus temperature were recorded.

The temperature corresponding to the $\tan\delta$ curve peak has been assumed as the value of T_g.

DMTA has been carried out for each hydrothermal conditioning, at three different stages of aging: *initial* (not aged samples), *saturated* (water uptake equilibrium), *desorbed* (at equilibrium).

2.4. Photoelastic Stress Analysis

Photoelastic Stress Analysis (PSA) is a well consolidated experimental technique able to provide full field maps of stresses [29]. In Transmission Photoelasticity, a transparent and birefringent material sample is positioned in series with other optical filters (all of which compose the Polariscope). Light, emitted by either monochromatic or white-light sources, travels through the polariscope, undergoing some wave transformations at the crossing of each optical element. In the case of a circular polariscope setup, the light intensity I coming out of the polariscope, and recorded by a digital photo-camera, is found to be related with the stress field by the following relationships [29,30]:

$$I(x,y) = I_o \sin^2(\pi\delta) \quad (2)$$

$$\delta = \frac{Cd}{\lambda}(\sigma_1 - \sigma_2) \quad (3)$$

So the light intensity is modulated over the sample surface as described by Eq. (2), forming a number of fringes. Equation (3) states that light intensity is in particular related to the difference of the in-plane principal stresses, σ_1-σ_2, through the calibration factor Cd/λ, where d is the sample thickness, λ the light wavelength, and C the photoelastic constant of the material [29].

In this work, a special configuration of circular polariscope is used, obtained by rotating the Analyser plate in the polariscope, and acquiring three images at three different orientations: Tardy Phase Shifting Method (TPSM) [30–32]. The combination of the three images allows for an effective measure of δ in eq. (1). Performing the unwrapping of the periodic δ, and rescaling by the calibration constant Cd/λ, provides the values of (σ_1-σ_2) along a chosen path in the sample. A detailed description of the analytical steps in the TPSM procedure can be found in Refs. [30,31].

In this work, the PSA and the TPSM are applied at different intervals in time, taking the aging samples out of the thermal bath and placing them in the polariscope for the photoelastic images acquisition. This procedure takes only few minutes, and was found to have no substantial influence on the water absorption kinetic [21,27]. All stored images where then post-processed and the TPSM applied along the vertical axis of symmetry from the edge ($y/W = 0$) to the centre ($y/W = 0.5$) of the rectangular samples (see Fig. 2), thus providing the stress *vs* time and stress *vs* position curves reported and commented in the results section.

By means of PSA, it is then possible to monitor the in-plane stress field evolution during the transitory stages of water diffusion and desorption, up to equilibriums. In particular, it has been found that the internal stresses detected by PSA arise due to the non-uniform material swelling that characterizes the transitory stages [21]. In particular, the entity and evolution of such stresses is believed to be dependent on the network structure of the material and its chemical interactions with the diffusing solvent [27].

3. Results and discussion

3.1. Properties before aging

In order to investigate the effects of ageing on the properties of the epoxy systems a preliminary characterisation was performed on unaged samples, as reference.

Curves of the storage modulus E' and loss factor $\tan\delta$ as function of the temperature are reported in Fig. 3. DMTA investigation of similar irradiated systems, cured in different irradiation conditions, has been carried out in Refs. [14,33], where the dynamic mechanical thermal behaviour is in particular correlated to the material fracture toughness [14], and to the molecular structure through solid state NMR analysis [33].

In accordance with the findings in Ref. [14], the present irradiated system DGEBFirr shows two well distinguishable relaxation peaks in the $\tan\delta$ curve, indicating a not uniform crosslinking degree, due to vitrification effects related to the low irradiation temperature. Such vitrification phenomena are overcome by the post-irradiation thermal treatment at a temperature value close to the first temperature peak. This treatment in fact, as shown in Fig. 3, causes the disappearing of the first peak [8,13], giving rise to a higher crosslinked and more uniform structure.

The different uniformity of the crosslinking density in the irradiated systems has been confirmed by solid state NMR analysis [33], which evidenced a correspondent different uniformity of the nuclear relaxation times.

In the same Fig. 3 the DMTA curves of the thermally cured sample is reported as comparison, showing a well defined

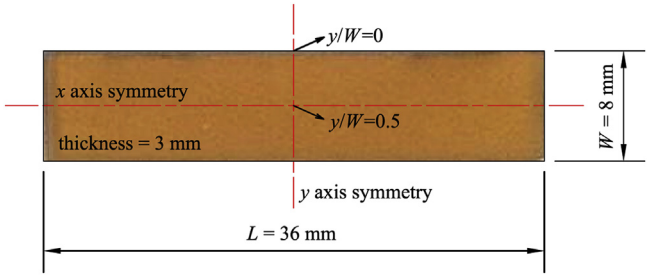

Fig. 2. Sample scheme.

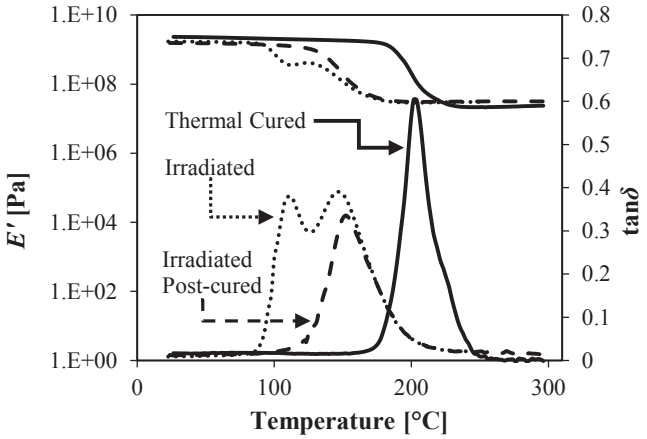

Fig. 3. DMTA curves at initial conditions (data relative to DGEBFt are derived from Ref. [27]).

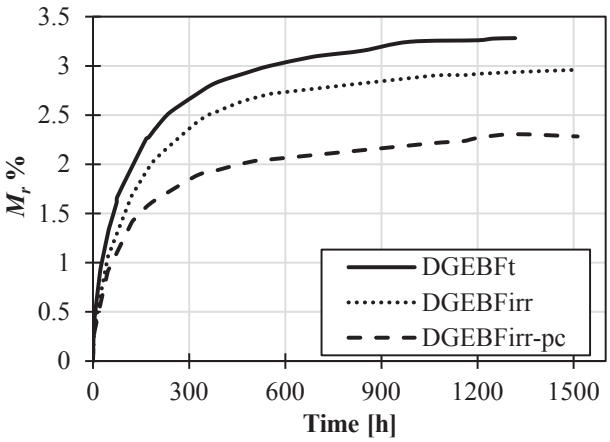

Fig. 4. Gravimetric curves during the absorption process (data relative to DGEBFt are derived from Ref. [27]).

relaxation at very high temperature, indicating a more uniform and more cross-linked system with respect to the irradiated systems.

In Table 1, both the temperatures and tanδ values, corresponding to the maximum value of tanδ curves, are reported. Looking at Table 1, both irradiated systems show a significant lower cross-linking density with respect to the thermally cured resin from Ref. [27]. This effect is due to the above mentioned vitrification phenomena, not entirely eliminated by post irradiation thermal curing, and to the different formulation between the irradiated and thermal systems. In fact, as already said in the experimental, the thermally cured system includes a tertiary ammine as curing agent [27] instead of the initiator used in the radiation curing.

3.2. Water uptake

The gravimetric curves are reported in Figs. 4 and 5 for the absorption and desorption process, respectively. The average values of M_r % measured on three nominally identical samples are reported. The standard deviation of all measured weights never exceeds 0.14% of the respective average weight, indicating a low data dispersion. Absorption values related to both saturated and desorbed equilibrium conditions are reported in Table 1.

It is noticeable that, at saturation, the irradiated systems show a lower absorption with respect to the thermally cured system. Previous work has suggested that a higher crosslink density, such as that of the thermal system, determines an intrinsically smaller chain mobility, causing a less compact system, and hence a higher free volume [4,16,34,35], which can explain the higher amount of absorbed water.

The different behaviour between DGEBFirr and DGEBFirr-pc can instead be related to a different chemical affinity with water. In fact DGEBFirr may have a higher amount of polar reactive groups, due to the presence of not-yet reacted epoxy groups together with other reactive groups formed during radiation curing, such as hydroxyl groups and frozen free radicals [1,14,36,37].

For each system, the diffusion coefficient D (diffusivity) is reported in Table 1, calculated by fitting experimental data with a Fick's second law model, assuming the last monitored values of water uptake as representative of the equilibrium condition [34]. Diffusivity indicates the rate by which absorbed/desorbed water approaches the equilibrium value in the initial stages of absorption/desorption, and as such, it can be seen as an indicator of the kinetics of reactions involving water uptake. The irradiated systems show a similar diffusivity, higher with respect to that of the thermally cured resin.

The desorption process, monitored up to the formation of a consolidated plateau, indicates the permanence of a significant residual water content in all systems (Fig. 5a–b and Table 1). The relative amount of residual (not-desorbed) water at desorption equilibrium, given by (M_{r_des}/M_{r_sat})%, is higher for DGEBFt, with a value of about 52%, while DGEBFirr and DGEBFirr-pc have respectively 38% and 27%. Desorption has been carried out at room temperature, activated by an external controlled dry airborne environment. Then it can be assumed that the desorbed water is mainly weekly bonded (or Type I) water and free water. Unlike the absorption process (which was favoured by higher temperatures), a general lower kinetics can now be observed, as also indicated by the desorption diffusivity values (Table 1). Moreover, the desorption process in the thermal system shows a slower diffusion coefficient (see Table 1), even though equilibrium is reached earlier, due to a higher residual water content with respect to the irradiated systems. In particular, DGEBFt reaches the equilibrium in desorption after about half time (3000 h) with respect to the irradiated systems [27].

The higher residual water in DGEBFirr with respect to DGEBFirr-pc can be attributed to the different affinity of the resin to chemically bond with water. In fact, as already discussed for the absorption process, the presence in DGEBFirr of more unreacted groups (epoxy and hydroxyl groups), makes it more prone to form type II multiple hydrogen bonds with water [22,24]. This makes the

Table 1
DMTA and gravimetric results for irradiated and thermal systems (for tanδ curves showing more than one peak, the value of each peak is indicated).

System	Temperature of tanδ peak [°C]	tanδ	Saturated condition M_{r_sat} %	Desorbed condition M_{r_des} %	Absorption Diffusivity D [cm^2/s]	Desorption Diffusivity D [cm^2/s]
Irradiated	114; 146	0.38; 0.40	2.96	1.12	2,72E-08	5,32E-09
Irradiated and thermally post cured	152	0.34	2.28	0.62	2,97E-08	8,77E-09
Thermally cured [27]	202	0.60	3.28	1.71	1,71E-08	1,45E-09

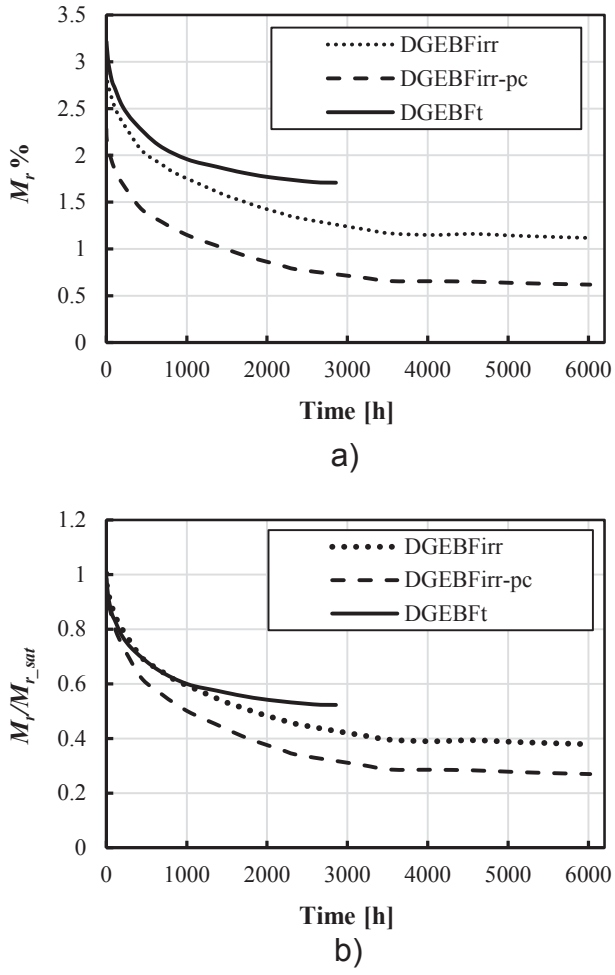

Fig. 5. Gravimetric curves of desorption process: a) relative mass out-take; b) relative mass outtake normalised by relative mass up-take at saturation (data relative to DGEBFt are derived from Ref. [27]).

desorption process at room temperature less effective, causing the higher residual water content in DGEBFirr.

In summary, regarding absorption, it can be said that the higher amount of absorbed water in DGEBFt, with respect to DGEBFirr and DGEBFirr-pc, is likely due to a higher amount of free water, favoured by a higher free volume. DGEBFirr is expected to have the higher amount of bonded water due to a better chemical affinity, and DGEBFirr-pc absorbs the least amount due to both smaller free volume and lower chemical affinity. Regarding water desorption at room temperature, the thermal system has the higher amount of water at equilibrium, that is likely immobilised free water [24]. For the irradiated systems, although DGEBFirr has more bonded water, it desorbs less than DGEBFirr-pc probably due to the presence of stronger bonds favoured by a higher amount of polar groups.

3.3. DMTA

The dynamic-mechanical analysis was also performed at the absorption plateau (*saturated*), and at the end of desorption (*desorbed*). All results are reported in Fig. 6. The tanδ peaks and the corresponding temperature values from DMTAs are reported in Table 2.

Looking at Fig. 6, plasticization/degradation effects are always observed after water absorption, evidenced by the shift of the tanδ curve towards lower temperatures. In particular, for the irradiated system a single tanδ peak in between the two peaks relative to the *initial* condition is found, indicating the formation of a more uniform crosslinked structure. This behaviour was already observed and described for similar systems formed by radiation cured blends of epoxy resins and PES thermoplastic, and has been interpreted with the increased mobility of the macromolecular chains, during ageing [11]. During absorption, the water molecules act as plasticizers for the polymeric chains with a double effect, the lowering of the crosslinking density of highly crosslinked clusters (plasticization), and the compacting of the network due to the completing of the cure reactions of the less crosslinked parts. This last effect can be attributed to both the increased mobility of the macromolecule chains and the mild thermal curing during ageing.

After desorption, the irradiated system maintains a single relaxation peak in the tanδ curve, at a temperature value slightly lower than the second peak of the *initial* condition, which is a further evidence of the irreversible completion of curing reactions occurring during the whole water absorption/desorption process. The peak at the desorption condition is at a temperature value higher than that of the saturated condition, according to the removal of part of the plasticizing water, and it remains slightly lower than the second peak of the *initial* condition.

Regarding the DGEBFirr-pc system, the decrease of the temperature corresponding to the relaxation peak after water absorption can be essentially related to plasticization effects. After desorption an almost complete recovery of the initial T_g can be observed.

A different behaviour characterizes DGEBFt (see Table 2, and the DMTA curves in Ref. [27]). It was observed that DGEBFt exhibits a relatively bigger drop of T_g, going from the initial to the saturation conditions. Furthermore, it forms a double peak at saturation, which is instead eliminated in the irradiated systems. Finally, at the end of desorption, a difference of about 30° remains between the tanδ peaks at the initial and the desorbed equilibrium condition, which is significantly bigger then the equivalent difference exhibited by the irradiated systems. Such more severe transformations in the tanδ curve of DGEBFt could be a consequence of the higher amount of water absorbed, and the less amount water desorbed by this system.

3.4. Photoelastic Stress Analysis

As already reported in Refs. [21,27], Photoelastic Stress Analysis (PSA) is a further characterisation that can be implemented during water absorption/desorption, to evaluate the average in-plane stress components as induced by non-uniform water concentration.

During the absorption stages preceding saturation, the outer zones of material near the sample surface develop a bigger swelling deformation, due to a higher amount of bonded water in these zones. Such swelling is restrained by the inner part of the sample, which has not yet been reached by water. This non-uniform deformation generates an internal self-equilibrated stress field, where the inner material develops traction along the beam main axis, while the outer material develops compression [21]. As water diffuses in the inner parts of the sample, and equilibrium is thus approached, swelling tends to reach a maximum, but also a more uniform distribution which de-facto reduces the internal constraint and thus relaxes the stresses. When the swelling becomes uniform due to a complete water uptake of the whole sample (saturation condition), stresses are also fully relaxed. In this condition, the sample is not un-strained, but uniformly swelled.

During desorption a similar rationale is followed. The outer zones of material release the absorbed water more rapidly than the inner sample. This generates a not uniform un-swelling, where the

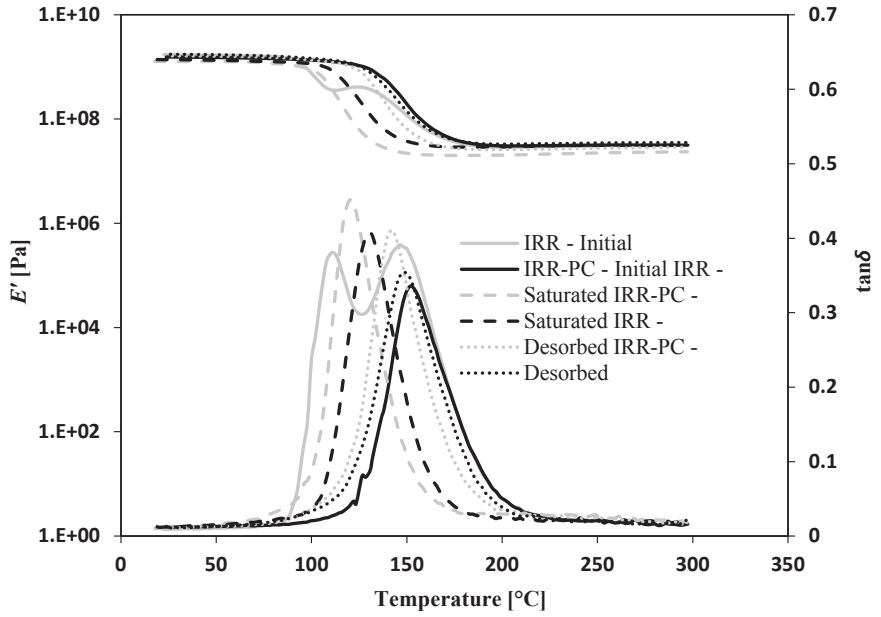

Fig. 6. DMTA curves in different conditions.

Table 2
Tanδ peaks and relative temperature values (for tanδ curves showing more than one peak, the value of each peak is indicated).

	DGEBFt [27]		DGEBFirr		DGEBFirr-pc	
	T_g [°C]	tanδ	T_g [°C]	tanδ	T_g [°C]	tanδ
Initial	202	0.6	112; 146	0.38; 0.39	152	0.34
Saturated	142; 168	0.41; 0.32	121	0.45	129	0.41
Desorbed	171	0.59	143	0.41	148	0.35

sample now get loaded in traction in the outer near-surface zones, and in compression in the inner zones. The quantitative TPSM analysis described in Sec. 2.4 has confirmed the above interpretation, by finding that the internal swelling stresses during desorption are opposite to those developed under absorption [21].

A quantitative analysis of the swelling stress versus time has been performed along the y-axis of symmetry (from the edge to the centre of the sample, see Fig. 2). The curves of σ_x versus time, relative to the centre of the sample ($y/W = 0.5$), are shown in Fig. 7 for absorption. The curves relative to the thermally cured sample from Ref. [27] are reported for comparison. In the figure, the tension values are presented towards time (Fig. 7a) and towards M_r/M_{r_sat} (Fig. 7b).

In both Fig. 7a–b, referred to the absorption stage, the central point of the sample remains always in traction along the x direction (positive tensions). All systems exhibit the same trend, with the maximum value reached at almost the same time.

It is noticed that the two post-cured systems exhibit a small swelling stress at time zero. Photoelasticity allowed to ascertain that such initial stress is due to the unavoidable small air humidity that these samples absorb after the post-cure, due to the strong dry condition left by the post-cure. Even so, this initial stress is rather small compared to the maximum stress reached during hydrothermal aging, and was reckoned as not influencing the trend behaviour observed between the three systems in the following aging history.

The kinetics of stress evolution in Fig. 7 is similar for all systems, while stress values are rather different. The curves relative to the

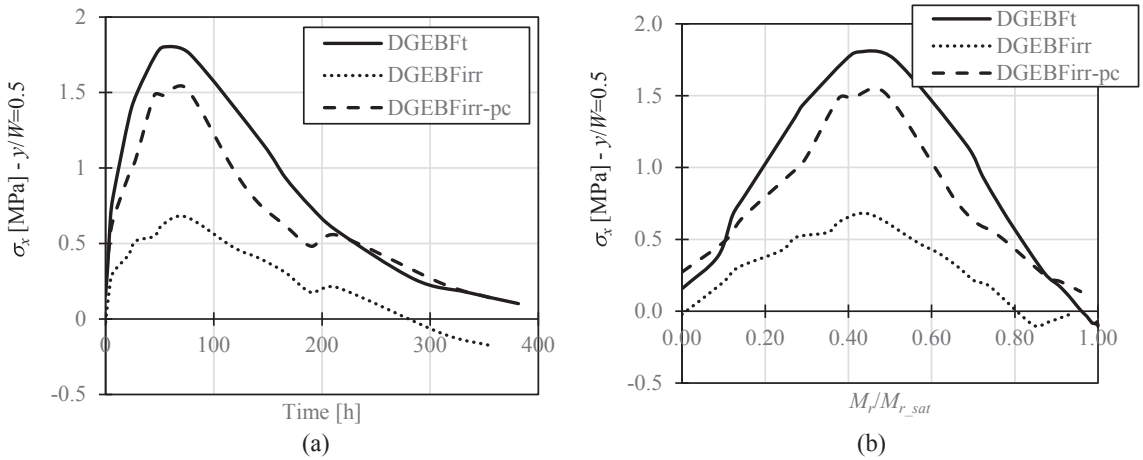

Fig. 7. Absorption process: hygroscopic stress versus: (a) time; (b) relative absorbed water (data relative to DGEBFt are derived from Ref. [27]).

irradiated systems are always below the one of the thermally cured system. In particular, DGEBFirr shows significant lower stress values. As previously said, stresses are induced by non-uniform swelling. In turn, swelling is believed to be mainly induced by bonded water [22,24,38]. The gravimetric data indicated that $DGEBF_t$ absorbs more water, but this was mainly composed by free water. It was also postulated that the irradiated systems somewhat favour bond water to free water, due to their higher chemical affinity, and smaller free volume. Therefore, it is plausible that the higher stresses in DGEBFt are rather related to its higher T_g (see Table 2), which suggests that this system is also more rigid in a mere mechanical sense.

The above rationale, i.e. higher network rigidity induces higher internal stresses, is still applicable to explain the differences between the two irradiated systems. In fact, DGEBFirr-pc has a higher stress than DGEBFirr, although the former absorbs a less amount of water. As commented in section 3.3, DGEBFirr develops a not uniform crosslinking density, witnessed by both lower T_g values and the presence of two relaxation peaks (see Fig. 6 and Table 2), while DGEBFirr-pc has a higher T_g and a single peak relaxation. This feature is an indication of a much higher internal mobility of the network in DGEBFirr, which translates in a higher compliance in terms of response to internal stresses.

Fig. 7b reveals also an interesting feature regarding the kinetics of hygroscopic stress evolution. The peak stress in the centre of the sample is reached when the relative amount of absorbed water, M_r, is about half the saturation value, M_{r_sat}. Moreover, the trend of stress vs relative water uptake is similar for all three systems.

The photoelastic analysis carried out along the y-axis of symmetry, and calculated at the time when the maximum hygroscopic stress occurs, is shown in Fig. 8. This figure confirms the lower stresses reached by the irradiated systems, with respect to the thermally cured one, also on the edge of the sample, where the stress component becomes negative (compression).

Furthermore, it is possible to observe that in DGEBFt the position of the neutral axis (i.e. the coordinate where the stress component σ_x is zero) is closer to the sample upper edge, while the peak compression stress is about twice bigger than that in the irradiated systems. These features confirm the intrinsically stiffer behaviour of DGEBFt with respect to the irradiated systems.

Analogues curves of the hygroscopic stress relative to the desorption transitory are reported in Figs. 9 and 10.

Fig. 9 shows that σ_x at the centre point, $y/W = 0.5$, is now always negative (i.e. compression). The three systems still exhibit a similar

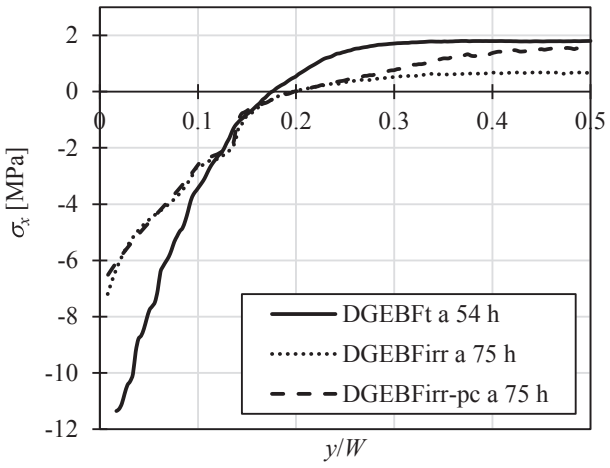

Fig. 8. Absorption process: hygroscopic stress along the y-axis (data relative to DGEBFt are derived from Ref. [27]).

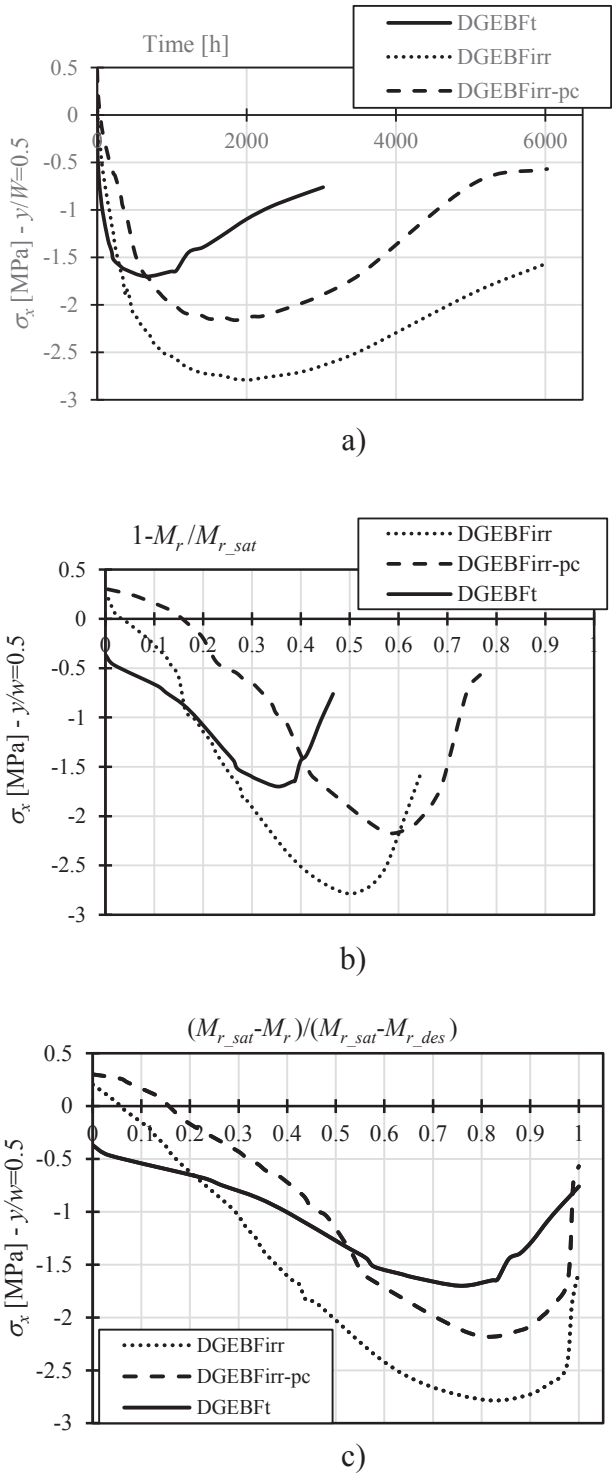

Fig. 9. Desorption process: hygroscopic stress versus: (a) time; (b) desorbed water relative to total absorbed water; (c) fraction of desorbed water. (Data relative to DGEBFt are derived from Ref. [27]).

trend, as in absorption, but with different values of the stress and, this time, also different kinetics. In particular, the irradiated systems now reach higher stress values than DGEBFt. Moreover, they seem to evolve significantly slower (see Fig. 9a).

The arising of a stress field in desorption is associated to the ability of the material to un-swell, mainly by relieving bonded water. It is found that the outer zones of material un-swell faster

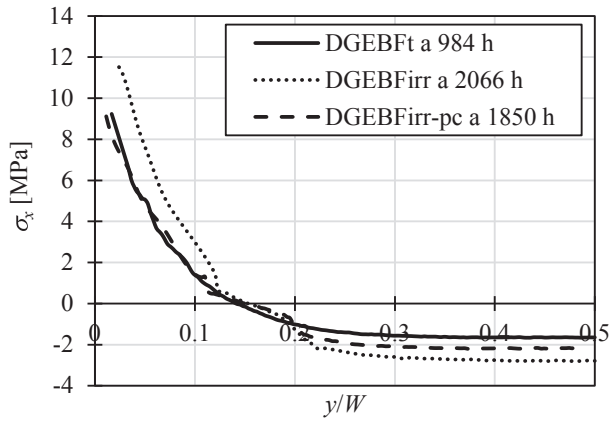

Fig. 10. Desorption process: hygroscopic stress along *y*-axis at desorption plateau. (Data relative to DGEBFt are derived from Ref. [27]).

due to the interaction with the dry airborne environment, thus compressing the material inner zones. A noteworthy result from Fig. 9 is that all three systems seem to still have a certain degree of residual compression at the reach of desorption equilibrium. This could be correlated with the difficulty of the samples to fully relieve all the bonded water (see also section 3.1), and in particular the bonded water in the inner parts of the sample, thus hampering a complete internal stresses relief. Fig. 9a also shows that after the peak formation, the stress has a much slower decay, compared to absorption, justified by the large difference of temperature of the two processes.

The irradiated systems exhibit also a significantly slower kinetics of stress evolution than DGEBFt, as shown in Fig. 9a. Fig. 9b plots the stress versus the amount of desorbed water, normalised by the total absorbed water. All systems have a similar trend, where it is clearly seen that the stress peak is achieved after most of the water is desorbed. This is better seen in Fig. 9c, where the stress is plotted versus the fraction of desorbed water. This plot is the equivalent for desorption of Fig. 7b. As in absorption, also in desorption the trend is similar, with the peak stress of all systems falling between 75 and 85% of desorbed water (this percentage was about 50% in absorption).

Another outcome from Fig. 9 is that, contrary to what found with absorption, the irradiated systems now reach a higher peak stress than DGEBFt. This is true for the centre point in compression, plotted in Fig. 9, but also for the traction at the border. Fig. 10 reports the hygroscopic stress along the *y*-axis of symmetry when the maximums occurs. The stress component σ_x near the edge is now positive (tensile), conversely to the absorption process, and the higher value of σ_x is still reached by DGEBFirr. The fact that such residual edge stresses in desorption are traction stresses of a quite significant amount should rise some concern. It means that the desorption processes might provide potential fracture energy to possible edge cracks present in the material [19].

The lower stresses developed by the thermal system during desorption could be due to its higher free volume, in part restored with the regaining of high T_g (see Table 2). Part of the released bonded water in the inner parts of the sample may transform into free water, remaining inside the material (which justifies also the least value of desorbed water found for DGEBFt). The loss of bonded water inside the sample would determine a certain unswelling of the kernel, thus reducing its constraint action towards the unswelling edges, and then helping to relax the whole stress field. Conversely, the DGEBFirr would release more bonded water from the sample edges, keeping a higher constraint with the unswollen kernel, which favours the reach of higher stresses. As already observed for absorption, the DGEBFirr-pc exhibits an intermediate behaviour, with peak stresses more comparable to DGEBFt, and an evolution that is more similar to DGEBFirr (see Figs. 9a and 10).

4. Conclusions

The present study, progressing from recent works [21,27], has confirmed the potentials of Photoelastic Stress Analysis (PSA) to evaluate hygroscopic stresses during water absorption/desorption of epoxy resin systems, which can retain transparent and birefringent properties after preparation. Ionizing irradiation curing is in particular considered, leading to not uniform cross-linking networks. Application of PSA has evidenced that absorption and desorption activates swelling induced internal stresses with significantly different features.

Combining the present results with those from equivalent thermally cured epoxies [27], it is confirmed a general trend that the swelling stresses during absorption increase with increasing material T_g. This could suggest that a more rigid network, associated to a higher T_g, reacts to the same swelling deformation with higher stresses. The rate of internal stress evolution during absorption, in samples with nominally identical dimensions, instead seems to be little influenced by the different materials properties such as T_g, water diffusivity and absorbed water at equilibrium.

Since swelling is mainly induced by bonded water, it is possible that the observed kinetic behaviour is due to the fact that the rate of bonded water formation in the studied systems is similar, regardless of the absolute amount of bonded water and the differences in water diffusivity.

Desorption at room temperature induces some peculiar behaviours, with a reverse in the sign of stresses arising from non-uniform material un-swelling. In particular, sample edges may develop traction stresses, providing potential fracture energy to edge cracks/notches. A significant amount of residual water at desorption equilibrium is also found, as well as the permanence of a residual stress field. This may confirm the existence of a type II bonded water, as well as trapped free water, which can be both difficult to expel out at room temperatures. Contrary to absorption, in desorption the higher hygroscopic stresses have been observed in systems with lower T_g, and this trend is common for the present irradiated systems and for the thermal systems of [27]. Furthermore, the kinetics of stress formation during desorption is now different (contrary to absorption), with thermally cured system showing a faster evolution.

Summarising on the findings for the DGEBF monomer based epoxies, from a mere stress behaviour, the irradiated plus thermally post-cured system, DGEBFirr-pc, exhibits probably the best compromise with respect to both pure irradiation (DGEBFirr) and pure thermal curing (DGEBFt). In fact, DGEBFirr-pc has low stresses in desorption (similarly to DGEBFt) while keeping a slow stress kinetics (similarly to DGEBFirr). It also has lower stresses in absorption (similarly to DGEBFirr) while keeping a relatively high T_g and a lower water absorption. These results evidence a great potentiality of e-beam irradiation as a suitable process to obtain epoxy systems for use as matrices in advanced materials such as carbon fibre composites in the field of aeronautic and aerospace applications.

References

[1] B. Ellis, in: Chemistry and Technology of Epoxy Resins, Springer Netherlands, Dordrecht, 1993, http://dx.doi.org/10.1007/978-94-011-2932-9.
[2] J.D. McCoy, W.B. Ancipink, C.M. Clarkson, J.M. Kropka, M.C. Celina, N.H. Giron, L. Hailesilassie, N. Fredj, Cure mechanisms of diglycidyl ether of bisphenol A (DGEBA) epoxy with diethanolamine, Polymer 105 (2016) 243–254, http://

dx.doi.org/10.1016/j.polymer.2016.10.028.
[3] M. Hesabi, A. Salimi, M.H. Beheshty, Effect of tertiary amine accelerators with different substituents on curing kinetics and reactivity of epoxy/dicyandiamide system, Polym. Test. 59 (2017) 344–354, http://dx.doi.org/10.1016/j.polymertesting.2017.02.023.
[4] S. Alessi, E. Caponetti, O. Güven, M. Akbulut, G. Spadaro, A. Spinella, Study of the curing process of DGEBA epoxy resin through structural investigation, Macromol. Chem. Phys. 216 (2015) 538–546, http://dx.doi.org/10.1002/macp.201400510.
[5] M.E. Launey, R.O. Ritchie, On the fracture toughness of advanced materials, Adv. Mater. 21 (2009) 2103–2110, http://dx.doi.org/10.1002/adma.200803322.
[6] F.-L. Jin, S.-J. Park, Thermal properties of epoxy resin/filler hybrid composites, Polym. Degrad. Stab. 97 (2012) 2148–2153, http://dx.doi.org/10.1016/j.polymdegradstab.2012.08.015.
[7] S. Masoumi, B. Arab, H. Valipour, A study of thermo-mechanical properties of the cross-linked epoxy: an atomistic simulation, Polym. Guildf. 70 (2015) 351–360, http://dx.doi.org/10.1016/j.polymer.2015.06.038.
[8] C. Dispenza, S. Alessi, G. Spadaro, Carbon fiber composites cured by γ-radiation-induced polymerization of an epoxy resin matrix, Adv. Polym. Technol. 27 (2008) 163–171, http://dx.doi.org/10.1002/adv.20127.
[9] S. Alessi, A. Parlato, C. Dispenza, M. De Maria, G. Spadaro, The influence of the processing temperature on gamma curing of epoxy resins for the production of advanced composites, Radiat. Phys. Chem. 76 (2007) 1347–1350, http://dx.doi.org/10.1016/j.radphyschem.2007.02.029.
[10] S. Alessi, C. Dispenza, P.G. Fuochi, U. Corda, M. Lavalle, G. Spadaro, E-beam curing of epoxy-based blends in order to produce high-performance composites, Radiat. Phys. Chem. 76 (2007) 1308–1311, http://dx.doi.org/10.1016/j.radphyschem.2007.02.021.
[11] S. Alessi, C. Dispenza, G. Spadaro, Thermal properties of e-beam cured epoxy/thermoplastic matrices for advanced composite materials, Macromol. Symp. 247 (2007) 238–243, http://dx.doi.org/10.1002/masy.200750127.
[12] G. Ranoux, M. Molinari, X. Coqueret, Thermo-mechanical properties and structural features of diglycidyl ether of BIS phenol a cationically cured by electron beam radiation, Radiat. Phys. Chem. 81 (2012) 1297–1302, http://dx.doi.org/10.1016/j.radphyschem.2011.12.009.
[13] G. Spadaro, S. Alessi, C. Dispenza, M.A. Sabatino, G. Pitarresi, D. Tumino, G. Przbytniak, Radiation curing of carbon fibre composites, Radiat. Phys. Chem. 94 (2014) 14–17, http://dx.doi.org/10.1016/j.radphyschem.2013.05.052.
[14] S. Alessi, D. Conduruta, G. Pitarresi, C. Dispenza, G. Spadaro, Hydrothermal ageing of radiation cured epoxy resin-polyether sulfone blends as matrices for structural composites, Polym. Degrad. Stab. 95 (2010) 677–683, http://dx.doi.org/10.1016/j.polymdegradstab.2009.11.038.
[15] S. Alessi, D. Conduruta, G. Pitarresi, C. Dispenza, G. Spadaro, Accelerated ageing due to moisture absorption of thermally cured epoxy resin/polyethersulphone blends. Thermal, mechanical and morphological behaviour, Polym. Degrad. Stab. 96 (2011) 642–648, http://dx.doi.org/10.1016/j.polymdegradstab.2010.12.027.
[16] O. Starkova, S.T. Buschhorn, E. Mannov, K. Schulte, A. Aniskevich, Water transport in epoxy/MWCNT composites, Eur. Polym. J. 49 (2013) 2138–2148, http://dx.doi.org/10.1016/j.eurpolymj.2013.05.010.
[17] M.R. Vanlandingham, R.F. Eduljee, J.W. Gillespie, Moisture diffusion in epoxy systems, J. Appl. Polym. Sci. 71 (1999) 787–798, http://dx.doi.org/10.1002/(SICI)1097-4628(19990131)71:5<787::AID-APP12>3.0.CO;2-A.
[18] P. Nogueira, C. Ramírez, A. Torres, M.J. Abad, J. Cano, J. López, I. López-Bueno, L. Barral, Effect of water sorption on the structure and mechanical properties of an epoxy resin system, J. Appl. Polym. Sci. 80 (2001) 71–80, http://dx.doi.org/10.1002/1097-4628(20010404)80:1<71::AID-APP1077>3.0.CO;2-H.
[19] G. Pitarresi, A. Toscano, M. Scafidi, M. Di Filippo, S. Alessi, G. Spadaro, Photoelastic Stress Analysis assisted evaluation of fracture toughness in hydrothermally aged epoxies, Frat. Ed. Integrita Strutt. 30 (2014) 127–137, http://dx.doi.org/10.3221/IGF-ESIS.30.17.
[20] G. Pitarresi, S. Alessi, D. Tumino, A. Nowicki, G. Spadaro, Interlaminar fracture toughness behavior of electron-beam cured carbon-fiber reinforced epoxy-resin composites, Polym. Compos. (2014), http://dx.doi.org/10.1002/pc.22806.
[21] G. Pitarresi, M. Scafidi, S. Alessi, M. Di Filippo, C. Billaud, G. Spadaro, Absorption kinetics and swelling stresses in hydrothermally aged epoxies investigated by photoelastic image analysis, Polym. Degrad. Stab. 111 (2015) 55–63, http://dx.doi.org/10.1016/j.polymdegradstab.2014.10.019.
[22] J. Zhou, J.P. Lucas, Hygrothermal effects of epoxy resin. Part I: the nature of water in epoxy, Polymer 40 (1999) 5505–5512, http://dx.doi.org/10.1016/S0032-3861(98)00790-3.
[23] M.J. Adamson, Thermal expansion and swelling of cured epoxy resin used in graphite/epoxy composite materials, J. Mater. Sci. 15 (1980) 1736–1745, http://dx.doi.org/10.1007/BF00550593.
[24] M.Y.M. Chiang, M. Fernandez-Garcia, Relation of swelling and Tg depression to the apparent free volume of a particle-filled, epoxy-based adhesive, J. Appl. Polym. Sci. 87 (2003) 1436–1444, http://dx.doi.org/10.1002/app.11576.
[25] M.B. Jackson, S.R. Heinz, J.S. Wiggins, Fluid ingress strain analysis of glassy polymer networks using digital image correlation, Polym. Test. 31 (2012) 1131–1139, http://dx.doi.org/10.1016/j.polymertesting.2012.08.007.
[26] G.M. Odegard, A. Bandyopadhyay, Physical aging of epoxy polymers and their composites, J. Polym. Sci. Part B Polym. Phys. 49 (2011) 1695–1716, http://dx.doi.org/10.1002/polb.22384.
[27] A. Toscano, G. Pitarresi, M. Scafidi, M. Di Filippo, G. Spadaro, S. Alessi, Water diffusion and swelling stresses in highly crosslinked epoxy matrices, Polym. Degrad. Stab. 133 (2016) 255–263, http://dx.doi.org/10.1016/j.polymdegradstab.2016.09.004.
[28] P. Fuochi, M. Lavalle, No title, in: Proc. Work. RADECS 2002, 19-20 Sept. 2002, pp. 209–212. Padova (Italy), n.d.
[29] K. Ramesh, Photoelasticity, in: W.N. Sharpe (Ed.), Springer Handb. Exp. Solid Mech., Springer US, Boston, MA, 2008, pp. 701–742, http://dx.doi.org/10.1007/978-0-387-30877-7_25.
[30] A. Ajovalasit, G. Petrucci, M. Scafidi, Measurement of edge residual stresses in glass by the phase-shifting method, Opt. Lasers Eng. 49 (2011) 652–657. http://dx.doi.org/10.1016/j.optlaseng.2011.01.004.
[31] M. Scafidi, G. Pitarresi, A. Toscano, G. Petrucci, S. Alessi, A. Ajovalasit, Review of photoelastic image analysis applied to structural birefringent materials: glass and polymers, Opt. Eng. 54 (2015), http://dx.doi.org/10.1117/1.OE.54.8.081206, 081206–081206.
[32] A. Ajovalasit, G. Petrucci, M. Scafidi, A critical assessment of automatic photoelastic methods for the analysis of edge residual stresses in glass, J. Strain Anal. Eng. Des. 49 (2014) 361–375, http://dx.doi.org/10.1177/0309324713515466.
[33] S. Alessi, A. Spinella, E. Caponetti, C. Dispenza, G. Spadaro, Structural investigation of e-beam cured epoxy resins through solid state NMR, Radiat. Phys. Chem. 81 (2012) 1328–1331, http://dx.doi.org/10.1016/j.radphyschem.2011.12.004.
[34] O. Starkova, S. Chandrasekaran, L.A.S.A. Prado, F. Tölle, R. Mülhaupt, K. Schulte, Hydrothermally resistant thermally reduced graphene oxide and multi-wall carbon nanotube based epoxy nanocomposites, Polym. Degrad. Stab. 98 (2013) 519–526, http://dx.doi.org/10.1016/j.polymdegradstab.2012.12.005.
[35] M. Jackson, M. Kaushik, S. Nazarenko, S. Ward, R. Maskell, J. Wiggins, Effect of free volume hole-size on fluid ingress of glassy epoxy networks, Polymer 52 (2011) 4528–4535, http://dx.doi.org/10.1016/j.polymer.2011.07.042.
[36] J.V. Crivello, Advanced curing technologies using photo- and electron beam induced cationic polymerization, in: Radiat. Phys. Chem., 2002, pp. 21–27, http://dx.doi.org/10.1016/S0969-806X(01)00476-5.
[37] J.W.T. Spinks, R.J. Woods, in: An Introduction to Radiation Chemistry, third ed., John-Wiley and Sons, Inc., New York, Toronto, 1990. ISBN 0-471-61403-3.
[38] X.J. Fan, S.W.R. Lee, Fundamental characteristics of moisture transport, diffusion, and the moisture-induced damages in polymeric materials in electronic packaging, in: X.J. Fan, E. Suhir (Eds.), Moisture Sensit. Plast. Packag. IC Devices, Springer US, Boston, MA, 2010, pp. 1–28, http://dx.doi.org/10.1007/978-1-4419-5719-1_1.